Pergamon

SCIENCE DIRECT®

Tetrahedron 59 (2003) 9555–9562

TETRAHEDRON

Simulation of 2D ^{1}H homo- and ^{1}H–^{13}C heteronuclear NMR spectra of organic molecules by DFT calculations of spin–spin coupling constants and ^{1}H and ^{13}C-chemical shifts

Carla Bassarello, Paola Cimino, Luigi Gomez-Paloma, Raffaele Riccio and Giuseppe Bifulco*

Dipartimento di Scienze Farmaceutiche, Università di Salerno, Via Ponte don Melillo I-84084 Fisciano (Salerno), Italy

Received 30 July 2003; revised 11 September 2003; accepted 2 October 2003

Abstract—Simulation of 2D ^{1}H homo- and ^{1}H–^{13}C heteronuclear NMR spectra of organic molecules are here suggested as a tool in the structure elucidation of organic compounds. DFT calculations of ^{1}H and ^{13}C chemical shifts are performed on a sample compound, the ethyl ester of the *exo*-2-norbornanecarbamic acid, with the mPW1PW91 method using the 6-31G(d) basis set, following a full optimization of the geometry. Homo and heteronuclear spin–spin coupling constants are also calculated, providing full prediction of the common 2D ^{1}H–^{1}H COSY, 2D ^{1}H–^{13}C HSQC, and 2D ^{1}H–^{13}C HMBC.

1. Introduction

The recent development of methods for quantum mechanical calculations of NMR parameters has guided the study of a wide range of chemical problems.[1,2] These have regarded mainly the most common NMR-active nuclei usually considered in structural chemistry, such as ^{31}P, ^{15}N, ^{1}H, ^{17}O and ^{13}C, and more recently this approach has investigated a number of less conventional nuclei.

GIAO chemical shift calculation[3] for organic molecules has recently emerged as one of the most promising new approaches in structure elucidation. In this regard, we have recently shown that the GIAO calculations of ^{13}C c.s. can be very helpful in the validation of low polarity rigid molecular structures[4] and for the determination of the relative configuration of flexible compounds.[5] Also, it has been shown that spin–spin coupling constant calculations at DFT level may be very useful for the comprehension of the multiplicity of the ^{1}H spectra of organic compounds and as a support in the interpretation of the NMR parameters necessary for extensive conformational analysis.[6–8] Moreover, we have recently compared different theory models and basis sets in the calculation of ^{13}C NMR chemical shifts of natural products in order to suggest a convenient and consistent protocol to be employed for the reproduction of the experimental ^{13}C spectra of organic molecules, by using different combinations of geometry optimization methods and single point ^{13}C chemical shift calculations, both using different theory levels and different basis sets.[9] In the present paper, we preliminarily investigated a strategy to be employed in the calculation of the ^{1}H chemical shifts of organic compounds, taking into consideration several natural products. Subsequently, we probed the possibility of obtaining calculated homo- and heteronuclear 2D NMR spectra, with the aim of suggesting a computational method able to provide results which can be directly interfaced with the data coming from the most common 2D NMR experiments used in the structure elucidation of organic molecules, and, ideally, from every kind of *n*D spectrum. Besides the obvious advantage of a direct comparison between the calculated NMR spectra of a candidate structure and its experimental counterpart, we must bear in mind the enormous advantage of spreading the correlation peaks over two or more dimensions. In fact, as we have previously pointed out,[4] c.s. calculation of the carbons, whose errors are relatively smaller in being extended over a large spectral width, may be much more helpful in supporting and understanding experimental data with regard to c.s. calculation of a nucleus the resonances of which are limited to narrower spectral ranges. By analogy, it is our intention to show here that calculated cross-peaks spread over two or more dimensions can allow a comparison with experimental data regulated by at least three parameters, i.e. the chemical shift values of two or more nuclei (in our cases both ^{1}H and ^{13}C), and, more importantly, the intensity of the cross-peaks, which is in turn regulated by the *J*-values involved in the magnetization transfer phenomenon on which the most of the *n*D experiments are founded. Moreover, the calculation of heteronuclear NMR experiments could allow a rapid assignment of the resonance of

Keywords: GIAO; ^{13}C NMR; ^{1}H NMR; DFT calculations; natural products; structure elucidation; *J*-couplings.
* Corresponding author. Tel.: +39-089-964353; fax: +39-089-962811; e-mail: bifulco@unisa.it

0040–4020/$ - see front matter © 2003 Elsevier Ltd. All rights reserved.
doi:10.1016/j.tet.2003.10.001

unknown natural and synthetic organic molecules based on the comparison of the relative position of the cross-peaks in the calculated and in the experimental 2D-experiment, with the aim of the spectroscopist avoiding the necessity of acquiring a large number of correlation experiments. The compound on which the calculations were performed was the ethyl ester of the *exo*-2-norbornanecarbamic acid (**1**). On this compound, that represents a medium weight organic molecule, were executed, for comparison, the 1D ^{1}H NMR spectrum, the 1D ^{13}C, the 2D $^{1}H-^{1}H$ COSY, the 2D $^{1}H-^{13}C$ HSQC, and the 2D $^{1}H-^{13}C$ HMBC spectra.

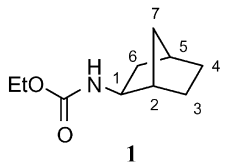

1

2. Results and discussion

2.1. Choice of the method for the GIAO calculations of ^{1}H and ^{13}C NMR chemical shifts

Prior to the calculation of the 2D NMR experiments for the test molecule used in our study, we took into consideration the necessity to obtain a fast and reliable protocol to be employed for the prediction of experimental ^{1}H and ^{13}C spectra of organic molecules. Following the strategies used in a previous paper that strictly concerns GIAO calculations of ^{13}C chemical shifts,[9] different combinations of geometry optimization methods and single point ^{1}H chemical shift calculations, both using different theory levels and different basis sets, were considered here. Aflatoxin β_1 (**2**), griseofulvine (**3**), magnolialide (**4**), benzofurano-eremophil-1-ene (**5**), and yohimbane (**6**) (Scheme 1) were used for the calculations, and the obtained values were compared to the reported ^{1}H chemical shifts[10–14] for the above compounds. Preliminary conformational searches for all compounds, by empirical force field molecular mechanics (MM) and dynamics (MD) calculations (see computational methods), were performed prior to QM geometry optimization.

As already observed for the ^{13}C c.s., also for the GIAO ^{1}H calculations, DFT methods show a very good agreement with the experimental results, and they usually perform better than the Hartree–Fock methods (Table 1). In particular, both the hybrid mPW1PW91[15] and B3LYP[16] functionals showed a satisfactory overlap between calculated and experimental ^{1}H c.s. values, and apparently the accuracy of the results increased on increasing the size of the basis set. These results are noticeably different to what was observed for ^{13}C, for which the best results, at a reasonable computational expense, were obtained with the 6-31G(d) basis set and the mPW1PW91 functional.[9] The geometry optimization level has been shown to affect the final results to a moderate extent, for both the ^{1}H and ^{13}C nuclei.

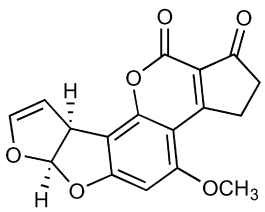

aflatoxin β1
2

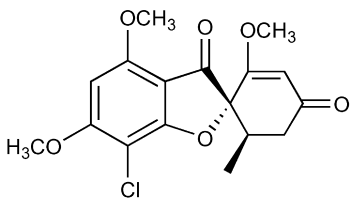

griseofulvine
3

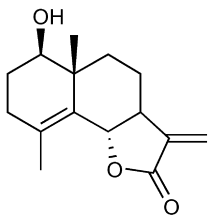

magnolialide
4

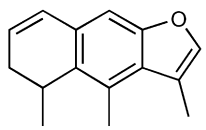

benzofurano-
eremophil-1-ene
5

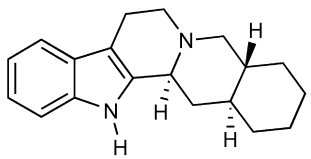

yohimbane
6

Scheme 1.

Table 1. R^2 (correlation coefficient), mean absolute error, mean error for different ^{1}H GIAO single point calculations//geometry optimizations

^{13}C GIAO single point calculation//geometry optimization	R^{2a}	MAE[b]	ME[c]
HF/6-31G(d)//HF/6-31G(d)	0.9757	0.28	0.23
HF/6-31G(d,p)//HF/6-31G(d)	0.9784	0.33	0.26
HF/6-311G(d)//HF/6-31G(d)	0.9736	0.27	0.20
HF/6-311G(d,p)//HF/6-31G(d)	0.9744	0.32	0.25
B3LYP/6-31G(d)//HF/6-31G(d)	0.9840	0.27	0.25
B3LYP/6-31G(d,p)//HF/6-31G(d)	0.9895	0.22	0.21
B3LYP/6-311G(d)//HF/6-31G(d)	0.9848	0.19	0.16
B3LYP/6-311G(d,p)//HF/6-31G(d)	0.9879	0.19	0.16
MPW1PW91/6-31G(d)//HF/6-31G(d)	0.9845	0.24	0.23
MPW1PW91/6-31G(d,p)//HF/6-31G(d)	0.9894	0.22	0.18
MPW1PW91/6-311G(d)//HF/6-31G(d)	0.9842	0.20	0.16
MPW1PW91/6-311G(d,p)//HF/6-31G(d)	0.9872	0.20	0.15
B3LYP/6-31G(d)//B3LYP/6-31G(d)	0.9871	0.23	0.19
B3LYP/6-31G(d,p)//B3LYP/6-31G(d)	0.9915	0.18	0.14
B3LYP/6-311G(d)//B3LYP/6-31G(d)	0.9878	0.16	0.10
B3LYP/6-311G(d,p)//B3LYP/6-31G(d)	0.9904	0.15	0.08
MPW1PW91/6-31G(d)//MPW1PW91/6-31G(d)	0.9877	0.19	0.15
MPW1PW91/6-31G(d,p)//MPW1PW91/6-31G(d)	0.9912	0.17	0.11
MPW1PW91/6-311G(d)//MPW1PW91/6-31G(d)	0.9871	0.17	0.08
MPW1PW91/6-311G(d,p)//MPW1PW91/6-31G(d)	0.9892	0.16	0.07

The calculated ^{1}H chemical shifts values were obtained by subtracting the ^{1}H isotropic magnetic shielding (IMS calculated by the GIAO method) from the average ^{1}H (IMS) of the tetramethylsilane (TMS): $\delta_{calcd}=|IMS_{TMS}-IMS_{xi}|$. A linear regression analysis was carried out taking into consideration the ^{1}H chemical shifts values, calculated (δ_{calcd}) for the optimized structures, versus the corresponding experimental ^{1}H chemical shifts values (δ_{exp}) reported in literature for the test compounds.[10–14]

[a] Correlation coefficient obtained by linear fitting of calculated (δ_{calcd}) versus experimental (δ_{exp}) ^{1}H NMR chemical shifts.

[b] MAE=mean absolute error=$\sum[|(\delta_{exp}-\delta_{calcd})|]/n$, sum of errors of experimental values from calculated ones, divided by the number of hydrogen atoms (n=77).

[c] ME=mean error=$\sum[(\delta_{exp}-\delta_{calcd})]/n$, sum of errors of experimental values from calculated ones, divided by the number of hydrogen atoms (n=77).

On the basis of the above considerations, and for a homogeneity of treatment for ^{1}H and ^{13}C, the geometry optimizations for our test compound has been executed at the mPW1PW91 level using the 6-31G(d) basis set, and, following, a single point calculation for the GIAO calculations of both ^{1}H and ^{13}C has been performed at the same level of theory. Also in this case, a preliminary conformational search, by empirical force field MM and MD calculations (see computational methods), was performed prior to DFT geometry optimization.

The results are reported in Table 2. The analysis of the mean absolute error for the ^{1}H (0.08 ppm), and for the ^{13}C nuclei (1.9 ppm), revealed an excellent reproducibility of the ^{1}H and ^{13}C spectra.

2.2. Determination of the spin–spin coupling constants

While the quantum mechanical calculation of chemical shifts for different nuclei has been extensively utilized in the last decade, only in the last few years have QM calculations of the J values attracted the attention of researchers. This has to be related with the recent introduction of experimental multi-dimensional NMR techniques that allow the measurement of coupling constants that are relevant to the study of different issues, such as conformational problems, stereochemical analysis, and detection of hydrogen bonds.

Table 2. Comparison of the calculated GIAO ^{1}H and ^{13}C NMR chemical shifts (at mPW1PW91 level using the 6-31G(d) basis set) and the experimental ^{1}H and ^{13}C (300, 75 MHz, $CDCl_3$, ppm relative to TMS) for compound **1**

^{1}H	Calculated	Experimental	^{13}C	Calculated	Experimental
1	3.56	3.48	1	53.7	54.3
2	2.21	2.19	2	43.7	42.7
3a	1.29	1.19	3	27.4	26.5
3b	1.55	1.46			
4a	1.14	1.09	4	29.3	28.3
4b	1.51	1.43			
5	2.08	2.24	5	36.4	35.8
6a	1.01	1.14	6	38.8	40.6
6b	1.77	1.75			
7a	1.25	1.15	7	35.5	35.3
7b	1.24	1.30			
CH_2	3.93	4.08	CH_2	58.9	60.6
Me	1.11	1.22	Me	14.9	14.8
			C=O	144.9	155.9

To calculate the ^{1}H–^{1}H and the ^{1}H–^{13}C coupling constants relative to our test compound, we have used the Gaussian 2003 software package,[17] which allows in a simple and direct manner to obtain what are considered the most relevant electron-nuclear interactions from which the spin–spin coupling phenomenon arises, i.e. the Fermi contact, the paramagnetic spin-orbit, the diamagnetic spin-orbit, and the spin-dipole terms. Since the FC term is very sensitive to electron correlation, a Hartree–Fock approach is to be excluded for satisfactory calculations of the J couplings. Moreover, among the post-HF methods, DFT has demonstrated, by a comparison among different levels of theory, a great efficiency in the calculation of the spin–spin couplings, even using basis sets of moderate size.[8] For these reasons, and in order to maintain an homogeneity relatively to the ^{1}H and ^{13}C calculations of the chemical shift of **1**, we have used the mPW1PW91 functional and the 6-31G(d) basis set for the spin–spin coupling computations. The so obtained results, listed in Table 3, may be considered pretty satisfactory, displaying a mean absolute error for the ^{1}H–^{1}H couplings of 0.3 Hz, and a mean error for the ^{1}H–^{13}C couplings of 1.5 Hz.

2.3. Simulation of the simplest 2D NMR spectrum: the ^{1}H–^{1}H COSY

Once we had obtained the complete prediction of the ^{1}H chemical shifts, and of the totality of the spin–spin coupling for **1**, they were used as an input (see computational methods) for the simulation of one of the most popular 2D spectra, i.e. the ^{1}H–^{1}H COSY. Though the first formulation of this experiment was published almost 30 years ago,[18] it is still one of the most used techniques in the structural elucidation of organic compounds, benefiting from diverse variations. It has to be pointed out that all the 2D spectra presented in this paper are not simple correlation plots in which the nuclei involved in the cross-peaks are reported; indeed, the simulations of all the NMR experiments were carried out by solving the exact solution of the Liouville equation, using the density matrix approach,[19,20] and

Table 3. Comparison between calculated (at mPW1PW91 level using the 6-31G(d) basis set) and experimental *J*-coupling values of compound **1**

	$^3J_{H-H}$			$^1J_{C-H}$			$^2J_{C-H}$			$^3J_{C-H}$	
	Calc.	Exp.		Calc.	Exp.		Calc.	Exp.		Calc.	Exp.
H1–H6a	2.8	2.4	C1–H1	148.5	147.6	C1–H6a	1.0	0.0	H1–C5	2.2	2.1
H1–H6b	8.5	8.1	C2–H2	136.4	142.6	C1–H6b	−3.5	−4.2	H2–C4	6.0	5.7
H2–H3b	4.6	4.2	C3–H3a	135.5	134.7	C2–H3b	−1.2	−2.7	H2–C5	8.4	5.3
			C3–H3b	132.0	132.1						
H5–H4b	4.2	4.1	C4–H4a	133.3	132.6	C2–H7a	−0.7	−2.0	H2–C6	4.8	3.6
			C4–H4b	131.8	131.6						
H5–H6a	4.4	4.2	C5–H5	131.8	141.8	C2–H7b	−0.6	−2.0	H4a-C2	2.1	2.4
			C6–H6a	131.4	128.0	C5–H4b	−1.2	−2.5	H5–C1	6.5	7.4
			C6–H6b	135.5	132.6						
			C7–H7a	133.0	133.6	C5–H6b	−1.3	−2.7	H–C═O	1.1	1.2
			C7–H7b	130.9	130.6						
			C–H (CH2)	144.5	146.8	C5–H7a	−0.7	−3.1			
			C–H (Me)	124.2	126.4	C5–H7b	−0.3	−1.8			
						C6–H2	−1.1	−1.3			
						C(Me)–H	−1.0	−2.3			
						$C(CH_2)$–H	−4.2	−4.2			

considering the Bloch equations for the relaxation phenomena[21] (Bruker NMR-Sim Software Package, version 3.0).[22] Also, the NMR-Sim software environment allows to simulate any kind of 1D and *n*D pulse sequence, and to set the parameters in complete analogy with regard to the experimental spectra. The experimental and the calculated 2D COSY spectra are depicted in Figure 1. The impressive similarities between the two spectra depend, in our opinion, on three main factors: (1) a good reproduction of the ^1H chemical shifts, which, as we have pointed out above, reveals a mean absolute error of 0.08 ppm, (2) the comparable relative intensities of the peaks, and (3) the shape of the peaks. Factors (2) and (3) are in turn related to the accuracy of $^1H-^1H$ spin–spin coupling calculation results, which indeed show a satisfactory mean absolute error (0.3 Hz). Particular attention has to be dedicated to the mentioned factors, being them responsible for the final appearance of the simulated 2D spectrum. In fact, while GIAO calculations of the chemical shifts have already shown to be of great support in the structure validation and in the stereochemical assignment of organic compounds,[4,5] the simulation of 2D NMR spectra of organic molecules possesses a much greater potential, being (a) directly comparable to the 2D experimental spectra; (b) carrying information on the *J*-coupling values, and so about the conformational and configurational features of the molecule under examination; (c) suggesting connections between the nuclei of a given molecule, and so providing validation tools upon comparison with the experimental spectra.

2.4. Simulation of the $^1H-^{13}C$ 2D HSQC spectrum

Together with the 2D COSY, one of the most straightforward techniques used in the structural determination of organic compounds is the direct $^1H-^{13}C$ heteronuclear correlation, whose most recent and popular applications, based on the inverse detection, are the HMQC and the HSQC. Again, we have represented the experimental and the calculated $^1H-^{13}C$ 2D HSQC in Figure 2. Also in this case, there is a clear-cut advantage with respect to the calculation of a 1D ^1H or a 1D ^{13}C spectrum: the suggestion or a validation of a methyl, a methylene, or a methyne in a

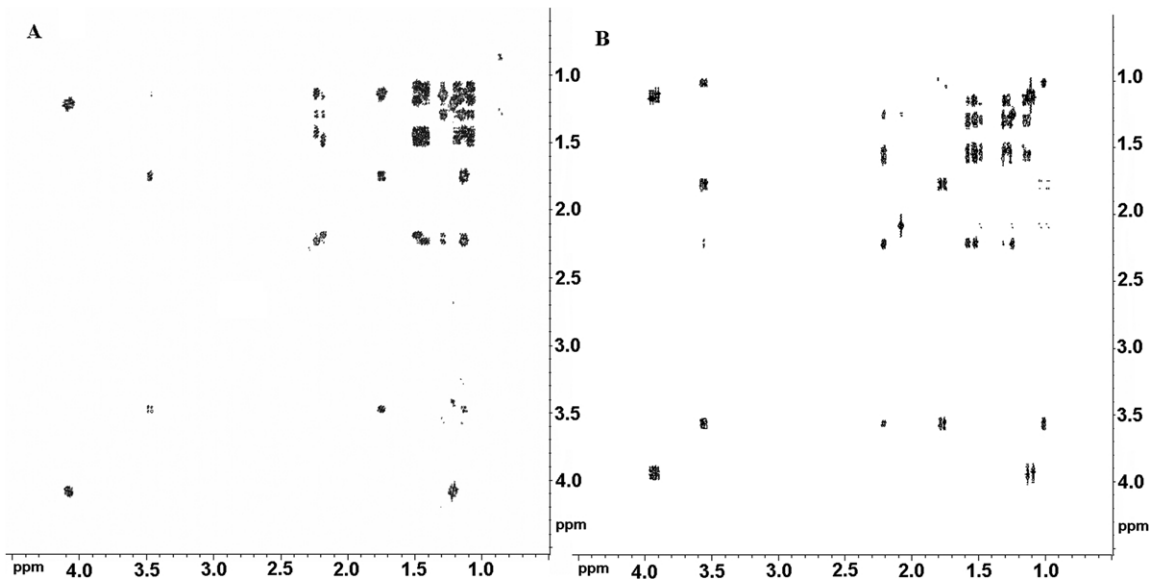

Figure 1. Comparison of the experimental (A) and calculated (B) 2D COSY.

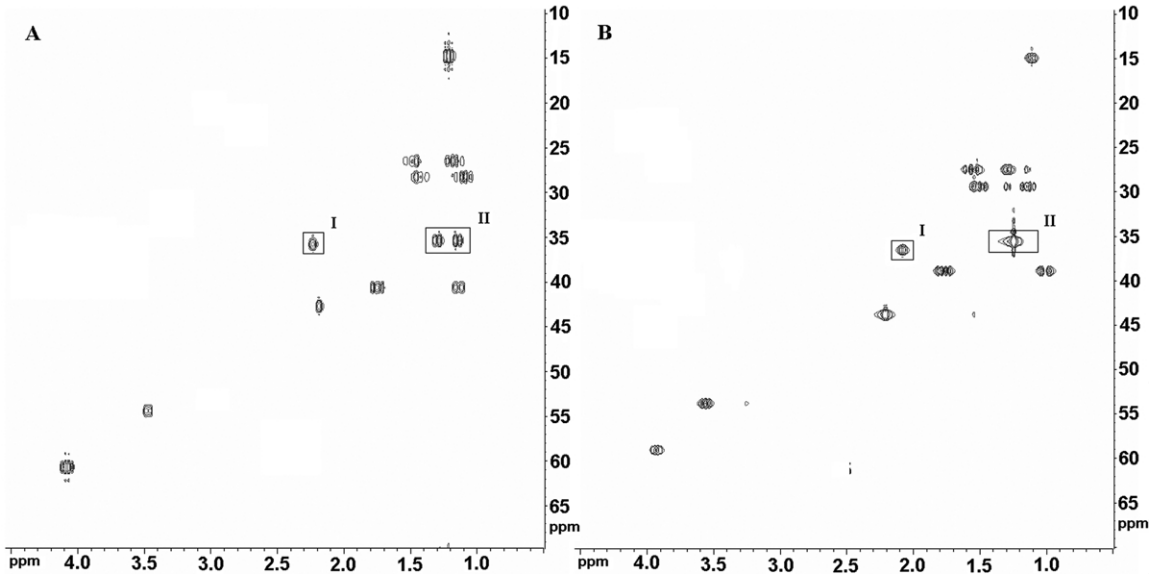

Figure 2. Comparison of the experimental (A) and calculated (B) ^{1}H decoupled 2D HSQC.

molecule is provided by the combinations of two c.s. parameters. Moreover, using the undecoupled version of the 2D HSQC (Fig. 3), we are able to observe and compare the calculated and the experimental direct ^{1}H–^{13}C coupling constants, which are very informative with regard to the kind of compound we are analyzing. An example are the $^{1}J_{CH}$ belonging to the ring of the norbornyl moiety of **1**, which all display characteristic values higher than 130 Hz. Considering that the average $^{1}J_{CH}$s for a five or a six-membered alicyclic compound are ca. 125–128 Hz (respectively), in our case the calculated J values could be crucial in a structural analysis, all being greater than 130 Hz and so excluding the presence of a five or six-membered ring and suggesting a bicyclic structure.

Another advantage in the reproduction of 2D heteronuclear experiments has been cited in the introduction: there is the possibility to obtain a rapid ^{1}H and ^{13}C assignment of unknown synthetic and organic products using this methodology. Indeed, the analysis of the calculated and the experimental 2D HSQC demonstrates that all the cross-peaks in the spectra, besides the very good agreement of the ^{1}H and ^{13}C values, are in the same relative positions. For this reason, a tentative identification of **1** made solely on the basis of a detailed comparison of calculated and experimental HSQC spectra, would afford the same result than we would have obtained by performing and interpreting extensive NMR spectroscopy (2D COSY, TOCSY, ROESY, HSQC, HMBC). Clearly, such a strategy of structure identification works best when only a very limited number of structural hypotheses are to be considered.

Moreover, in HSQC spectra, differently from what was observed in the COSY spectra, small differences are detectable between the experimental and calculated data, thanks to the better spreading of the cross-peaks along the

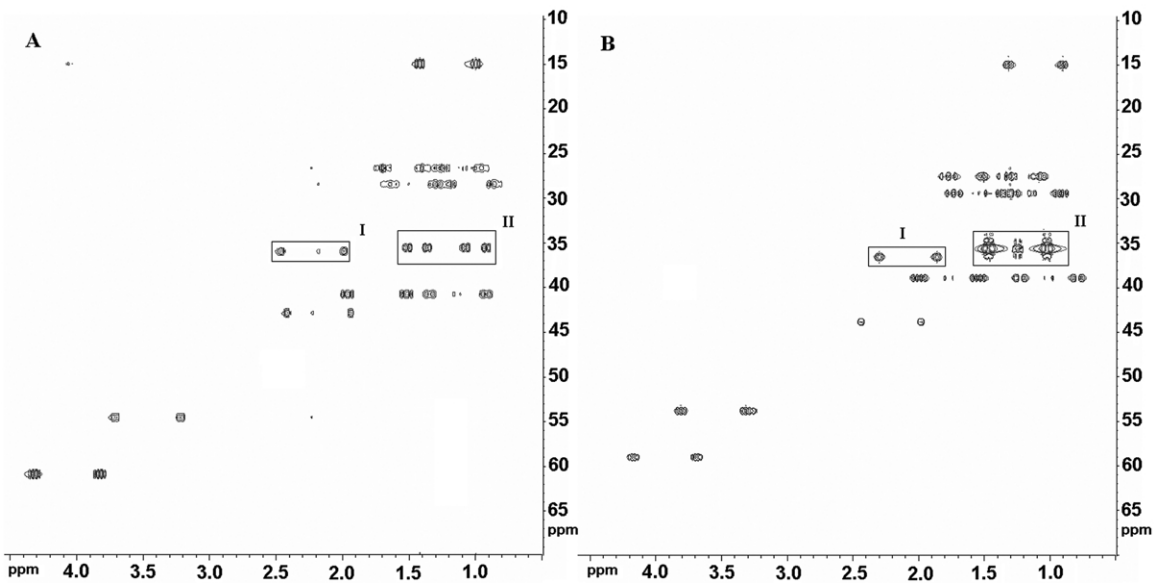

Figure 3. Comparison of the experimental (A) and calculated (B) ^{1}H coupled 2D HSQC.

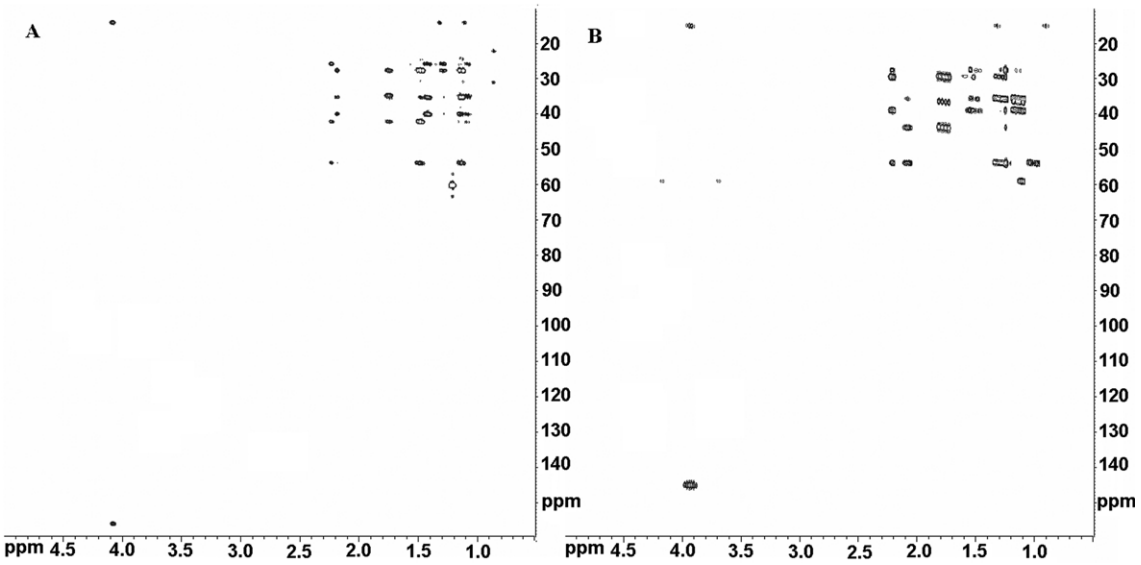

Figure 4. Comparison of the experimental (A) and calculated (B) 2D HMBC.

^{13}C dimension. In particular, predicted correlation peak H5/C5 (square box I, Fig. 2(B)) is, compared to the experimental analogous (square box I, Fig. 2(A)), upfield shifted with respect to the ^{1}H dimension. Also, a degeneration of protons H7a and H7b occurs in the predicted spectra, as observable in the relative correlation peaks H7a/C7 and H7b/C7 (square box II, Fig. 2(A) and square box II, Fig. 2(B), respectively). Analogous observations can be done for coupled 2D HSQC (square boxes I and II, Fig. 3(A) and square boxes I and II, Fig. 3(B)), in which the low reproducibility of the cited cross-peaks depends again on the chemical shift calculations and only slightly on the accuracy of the calculated *J*-values. These observations reveal that, while a good accuracy in the reproduction of the chemical shifts of both ^{1}H and ^{13}C may provide an extraordinary power to this technique, some failure may derive from the use of inadequate theory levels.

2.5. Simulation of the ^{1}H–^{13}C 2D HMBC spectrum

A simulation of the 2D HMBC spectrum, an inverse detection ^{1}H–^{13}C heteronuclear correlation which is widely used and it is of primary interest in the structure elucidation of natural and synthetic organic compounds, is also presented in this paper. In Figure 4 it is demonstrated how the experimental spectrum of **1** is excellently reproduced by our calculations, provided some differences as already described for the 2D HSQC. The 2D HMBC is an experiment of enormous interest because of its informative content: the correlation of hydrogens and carbons that are separated by two or three bonds, information necessary to connect the fragments obtained from the analysis of other spectra such as COSY and/or HSQC. Nevertheless the NMR spectroscopist is hardly able to predict or even justify a posteriori the presence, the absence, or the diverse intensities of HMBC correlations. Again, it has to be recalled that the intensities of the cross-peaks depend upon complex multiple *J*-modulated effects related to spin–spin couplings relative to the couple of nuclei involved in the correlation. This in turn is related to the conformational arrangement of the molecule. It is for this reason that our protocol, which involves a step of full geometry optimization prior to the chemical shift and the *J*-coupling calculation, is particularly efficient in reproducing the ^{2}J and the ^{3}J values, and so the intensities of the cross-peaks in an HMBC experiment.

3. Conclusions

A full quantum mechanical simulation of the most common homonuclear and heteronuclear 2D NMR experiments, executed with a moderate computational demanding level of theory (mPW1PW91/6-31G(d) for both geometry optimization and single point calculation of the NMR parameters), has demonstrated a good to excellent agreement between the experimental and calculated 2D COSY, 2D HSQC, and 2D HMBC for a test organic compound (ethyl ester of the *exo*-2-norbornanecarbamic acid). This study has highlighted the possibility to directly and visually compare calculated NMR parameters coming from quantum mechanical calculations with the experimental data acquired on an organic compound of medium molecular weight. In this case, the information content associated with the above experiments, has allowed the comparison, besides the ^{1}H and ^{13}C parameters, of the ^{1}H–^{1}H and ^{1}H–^{13}C connectivities obtained by means of the calculated *J* values. Moreover, following this methodology, the possibility of obtaining a rapid ^{1}H and ^{13}C assignment of unknown synthetic and organic products through a comparison of the experimental and calculated spectra has been clearly demonstrated. The only limit of the methodology may be related to the level of theory used for the calculations, which may cause a low reproducibility in selected cross-peaks; on the other hand, an increase in the effectiveness of the technique may be achieved choosing the adequate level of theory for the system under examination, fittingly the available calculation power.

4. Experimental

4.1. NMR measurements

NMR measurements were performed at 300 K on a Bruker DRX-600 and a Bruker Avance-300 spectrometers operating at 600 and 300 MHz, respectively. All the spectra except the 2D HMBC were acquired in the phase-sensitive mode, and TPPI method was used for quadrature detection in the indirect dimension.

The sample of the ethyl ester of the *exo*-2-norbornanecarbamic acid (**1**) was prepared by dissolving 35 mg in 0.5 mL of $CDCl_3$ (Carlo Erba, 99.95% D).

A total of 8 scans/t_1 value were acquired on the Bruker DRX-600 spectrometer for the phase-sensitive COSY[18] (t_{1max}=96.9 ms) spectrum. The HMBC[23] spectrum was executed on the Bruker DRX-600 spectrometer recording a total 16 scans/t_1 with a t_{1max} of 7.3 ms, Δ=50 ms.

The decoupled and coupled HSQC[24] experiments were executed on the Avance 300 spectrometer recording a total 16 scans/t_1 (t_{1max} of 13.0 ms) and 16 scans/t_1 (t_{1max} of 24.3 ms), respectively.

$^3J_{H-H}$ values were extracted from 1D ^{1}H NMR. $^{2,3}J_{C-H}$ values were obtained from phase-sensitive PFG-HETLOC and phase-sensitive PFG-PS-HMBC spectra according to the following conditions.

The PFG-HETLOC[25] spectrum was executed on the Bruker DRX-600 spectrometer recording a total of 32 scans/t_1 value (t_{1max} 16.4 ms). The MLEV-17 spin-lock period, including a trim pulse (2.5 ms), was set for 50 ms. The Δ in the half-filter was set at 3.75 ms which was optimized for CH/CH_2 and CH_3 while the BIRD inversion recovery delay at 400 ms.

The PFG-PS-HMBC spectrum was recorded on the Bruker DRX-600 spectrometer with the delay (Δ) set at 50 ms and 32 scans/t_1 value (t_{1max} 14.5 ms).[26,27]

NMR data were processed on a Silicon Graphic Indigo2 workstation using the Bruker XWIN-NMR software.

4.2. Computational details

MM/MD calculations on each of the compounds under examination were performed on Silicon Graphics Indigo2 using the CVFF force field[28] and the INSIGHT II/Discover package.[29] MD calculations (500 K, 50 ps) were executed in order to allow a full exploration of the conformational space. The Verlet algorithm was used to integrate the equation of motions. The chloroform solution phase was mimicked through the value of the corresponding dielectric constant. All the structures so obtained were minimized using the steepest descent and Newton–Raphson algorithms (maximum derivative less than 0.05 kcal/mol). This led to the selection of the lowest energy minimum conformers. The geometry of the above, as well as that of tetramethylsilane (TMS), was subsequently optimized at HF and/or DFT level.

QM calculations were carried out using the Gaussian03W program package.[17] For the preliminary analysis, relative to the choice method for the ^{1}H chemical shifts calculations, structures and energies of the considered species were optimized at HF and DFT (B3LYP and mPW1PW91) level using the 6-31G(d) basis set. The ^{1}H c.s. calculations of the optimized geometries were performed using HF and DFT methods. In the latter, the B3LYP and mPW1PW91 functional has been employed. For each of the approaches considered the 6-31G(d), 6-31G(d,p), 6-311G(d) and 6-311G(d,p) basis sets were utilized. The calculated values of chemical shift were referred to the theoretical tetramethylsilane ^{13}C c.s. value, computed at the same level of theory.[30,31] To test the different theoretical approaches here reported, computed and experimental[10–14] ^{1}H chemical shifts of the considered molecules were compared.

For the test compound **1** (ethyl ester of the *exo*-2-norbornanecarbamic acid), GIAO ^{1}H and ^{13}C calculations were performed using the mPW1PW91 functional and the 6-31G(d) basis set, using as input the geometry previously optimized at mPW1PW91/6-31G(d) level. The same methods were employed to calculate the spin–spin coupling values.

All the calculations of the 2D spectra, based on the NMR parameters obtained in the above manner, have been performed using the Bruker NMR-Sim 3.0 program.[22] As already pointed out briefly in Section 2.3, the time evolution of the density matrix, used to describe the spin system, was implemented by the program solving the Liouville equation of motion. The Hamiltonian governing the development of the density matrix is numerically calculated through the propagator U. The exact evolution of the whole spin system during all pulses is taken into account, without approximations resulting from analytical formulas or simplifications. Moreover, the program allows to carry out sequences with phase cycle because the propagators for radio-frequency pulses are phased using the appropriate phase specified by the pulse sequence. The effect of the whole pulse program is simulated by numerical calculation of the product of all the interval propagators contained in the sequence. As concerning the relaxation phenomena, NMR-Sim neglects the relaxation effects during radio-frequency pulses, while it uses the Bloch equation for the relaxation of longitudinal magnetization.

The spectrum is generated loading the pulse program and the spin system of the molecule under examination. The pulse program is the same as that implemented experimentally: all the necessary parameters are set (spectral width, pulse length, scans, relaxation time and so on).

The spin system is defined inserting all the chemical shifts of the proton and carbon nuclei, and, with respect to the desired sequence, the corresponding J values. Both chemical shifts and J values were derived from Gaussian's outputs obtained following the above procedures. All the isolated spin systems have been considered separately. For the heteronuclear spectra $^3J_{H-H}$ values less than 1.0 Hz have been neglected.

References

1. de Dios, A. C. *J. Prog. Nucl. Magn. Reson. Spectrosc.* **1996**, *29*, 229–278.
2. Helgaker, T.; Jaszunski, M.; Ruud, K. *Chem. Rev.* **1999**, *99*, 293–352.
3. Wolinski, K.; Hinton, J. F.; Pulay, P. *J. Am. Chem. Soc.* **1990**, *112*, 8251–8260.
4. Barone, G.; Gomez-Paloma, L.; Duca, D.; Silvestri, A.; Riccio, R.; Bifulco, G. *Chem. Eur. J.* **2002**, *8*, 3233–3239.
5. Barone, G.; Duca, D.; Silvestri, A.; Gomez-Paloma, L.; Riccio, R.; Bifulco, G. *Chem. Eur. J.* **2002**, *8*, 3240–3245.
6. Taehtinen, P.; Bagno, A.; Klika, K. D.; Pihlaja, K. *J. Am. Chem. Soc.* **2003**, *125*, 4609–4618.
7. Cloran, F.; Carmichael, I.; Serianni, A. S. *J. Am. Chem. Soc.* **2001**, *123*, 4781–4791.
8. Bagno, A. *Chem. Eur. J.* **2001**, *7*, 1652–1661.
9. Cimino, P.; Gomez-Paloma, L.; Duca, D.; Riccio, R.; Bifulco, G. *J. Mol. Struct.* (*Theochem*), submitted for publication.
10. Mao, H.; Deng, Z.; Wang, F.; Harris, T. M.; Stone, M. P. *Biochemistry* **1998**, *37*, 4374–4387.
11. Liu, Z.; Chen, H.; Jia, Z.; Dalley, N. K.; Hou, X.; Li, D.; Owen, N. L.; Grant, D. M. *Phytochemistry* **1995**, *40*, 1191–1192.
12. Kisiel, W.; Zielińska, K. *Phytochemistry* **2001**, *57*, 523–527.
13. Aubé, J.; Ghosh, S.; Tanol, M. *J. Am. Chem. Soc.* **1994**, *116*, 9009–9018.
14. Arison, B. H.; Wendler, N. L.; Taub, D.; Hoffsommer, R. D.; Kuo, C. H.; Slates, H. L.; Trenner, N. R. Contribution from the Merck Sharp & Dohme Research Laboratories, Merck & Co., Inc.: Rahway, NJ, 5 March, 1963.
15. Adamo, C.; Barone, V. *J. Chem. Phys.* **1998**, *108*, 664–675.
16. Becke, A. D. *J. Chem. Phys.* **1993**, *98*, 5648–5652.
17. Frisch, M. J.; Trucks, G. W.; Schlegel, H. B.; Scuseria, G. E.; Robb, M. A.; Cheeseman, J. R.; Montgomery, J. A., Jr.; Vreven, T.; Kudin, K. N.; Burant, J. C.; Millam, J. M.; Iyengar, S. S.; Tomasi, J.; Barone, V.; Mennucci, B.; Cossi, M.; Scalmani, G.; Rega, N.; Petersson, G. A.; Nakatsuji, H.; Hada, M.; Ehara, M.; Toyota, K.; Fukuda, R.; Hasegawa, J.; Ishida, M.; Nakajima, T.; Honda, Y.; Kitao, O.; Nakai, H.; Klene, M.; Li, X.; Knox, J. E.; Hratchian, H. P.; Cross, J. B.; Adamo, C.; Jaramillo, J.; Gomperts, R.; Stratmann, R. E.; Yazyev, O.; Austin, A. J.; Cammi, R.; Pomelli, C.; Ochterski, J. W.; Ayala, P. Y.; Morokuma, K.; Voth, G. A.; Salvador, P.; Dannenberg, J. J.; Zakrzewski, V. G.; Dapprich, S.; Daniels, A. D.; Strain, M. C.; Farkas, O.; Malick, D. K.; Rabuck, A. D.; Raghavachari, K.; Foresman, J. B.; Ortiz, J. V.; Cui, Q.; Baboul, A. G.; Clifford, S.; Cioslowski, J.; Stefanov, B. B.; Liu, G.; Liashenko, A.; Piskorz, P.; Komaromi, I.; Martin, R. L.; Fox, D. J.; Keith, T., Al-Laham, M. A.; Peng, C. Y.; Nanayakkara, A.; Challacombe, M.; Gill, P. M. W.; Johnson, B.; Chen, W.; Wong, M. W.; Gonzalez, C.; Pople, J. A. *Gaussian 03W*, *Revision 6.0*; Gaussian, Inc., Pittsburgh PA, 2003.
18. Aue, W. P.; Bartholdi, E.; Ernst, R. R. *J. Chem. Phys.* **1976**, *64*, 2229–2246.
19. Abragam, A. *The Principles of Nuclear Magnetism*; University: Oxford, 1961.
20. Slichter, C. P. *Principles of Magnetic Resonance*; Springer: Berlin, 1978.
21. Bloch, F. *Phys. Rev.* **1957**, *105*, 1206–1222.
22. Bruker Analytic GmbH. *NMR-Sim software Manual*, version 3.0, 2001.
23. Bax, A.; Summers, M. F. *J. Am. Chem. Soc.* **1986**, *108*, 2093–2094.
24. Burum, D. P.; Ernst, R. R. *J. Magn. Reson.* **1980**, *39*, 163–168.
25. Uhrín, D.; Batta, G.; Hruby, V. J.; Barlow, P. N.; Kövér, K. E. *J. Magn. Reson.* **1998**, *130*, 155–161.
26. Boyd, J.; Soffe, N.; John, B.; Plant, D.; Hurd, R. *J. Magn. Reson.* **1992**, *98*, 660–664.
27. Davis, A. L.; Keeler, J.; Laue, E. D.; Moskau, D. *J. Magn. Reson.* **1992**, *98*, 207–216.
28. Dauber-Osguthorpe, P.; Roberts, V. A.; Osguthorpe, D. J.; Wolff, J.; Genest, M.; Hagler, A. T. *Proteins: Struct. Funct. Genet.* **1988**, *4*, 31–47.
29. Accelrys Inc. (US, U.K.) 9685 Scranton Rd, San Diego, CA, 92121-3752.
30. Ditchfield, R. *Mol. Phys.* **1974**, *27*, 789–807.
31. Rohlfing, C. M.; Allen, L. C.; Ditchfield, R. *Chem. Phys.* **1984**, *8*, 9–15.